PERFORMANCE ANALYSIS OF AN ORGANIC RANKINE CYCLE FOR INTEGRATION IN A CARNOT BATTERY

Aditya Pillai[1*], Alihan Kaya[1], Michel De Paepe [1], Steven Lecompte [1]

[1] Ghent University, Department of Flow, Heat and Combustion Mechanics,
9000 Ghent, Belgium
aditya.pillai@ugent.be

* Corresponding Author

ABSTRACT

The purpose of this study is to report the challenges associated with the design of an ORC setup to be connected to a power-heat-power system, also known as a Carnot battery. Power is converted to heat using a high-temperature heat pump (HT-HP) and is stored using a separate sensible and latent heat storage system, consisting respectively of a phase change material (PCM) i.e., molten salt and pressurized hot water. Simulations are carried out in Python and Engineering Equation Solver (EES) to investigate the effect of the two storage systems on the performance of the ORC considering different working fluids. Working fluids that have low global warming potential (GWP) and zero ozone depleting potential (ODP) are considered. Minimizing irreversibilities during pre-heating and evaporating is of key importance. The identified working fluids of interest are HFO-1336mzz(E) & R1234ze(Z). The exergy destruction in the ORC increases by 73% if R1234ze(Z) is used as the working fluid. Finally, based on the acquired results, a preliminary test-rig is developed with a volumetric piston expander. The net power output from the test-rig is estimated to be approximately 10 kWe.

1. INTRODUCTION

With an ever growing concern about the environment and increasing awareness to curb global warming and climate change, attention has now shifted towards methods of energy generation using renewable sources. The challenge faced when attempting to integrate renewable energy sources in the grid is the intermittent nature of the supply of energy and the difficulty in matching supply to demand. Energy storage systems prove to be a solution in tackling these problems. To completely transition to an energy system that is based on renewable energy sources (RES), energy storage systems play a vital role Denholm & Hand (2011); Inage (2015).

The main electrical energy storage (EESt) technologies today are Pumped Hydro Energy Storage (PHES) and Compressed Air Energy Storage (CAES) systems. The most economical option to store large amounts of electrical energy is the PHES system Akhil *et al.* (2013). This technology is heavily restricted by geographical requirements, locations of easy extraction in Europe have already been exploited Gutiérrez & Arántegui (2015) and have high investment costs IRENA (2012).

The diabatic CAES system, as the name suggests, works by storing compressed air high pressure in pressure vessels. These CAES system are the only ones commercially available in the market. Being dependent on fossil fuel is huge drawback for such systems.

EESt are very promising, efficient and reliable technologies and utilization of RES to a greater degree is possible on their employment Gallo *et al.* (2016); Connolly *et al.* (2012). Energy storage systems allow for closer incorporation of RES in the grid by providing auxiliary control over the voltage or primary control reserve Müller *et al.* (2017), which would not be feasible if the source were photo voltaic cells or wind power plants.

An emerging and lucrative method for large scale energy storage system is the Pumped Thermal Energy Storage (PTES), alternatively known as a Carnot battery. The basic concept behind a PTES system is to use a power-to-heat system to store electrical energy in a thermal energy reservoir (which could be a latent heat storage, sensible heat storage or both), and then use this heat at high temperature to drive a heat engine to produce electricity and optionally, heating at lower temperatures. Although the efficiency of thermal engines for producing electricity is quite low Zhu (2015), the combined heat pump and heat engine system are much more attractive.

The PTES system can be classified based on the thermodynamic cycle they operate on. It may follow, amongst others, a Brayton cycle, a CO_2 supercritical Rankine cycle or an organic Rankine cycle. Steinmann Steinmann (2014) presented the Compressed Heat Energy Storage (CHEST) concept which operated on a Rankine cycle with latent TES. The system obtained an efficiency of 70%, but it was shown that the integration of a low temperature heat source, like those obtained from waste heat sources or solar thermal energy, might reduce losses resulting from the irreversibility as a consequence of heat transfer between the available low temperature heat source and heat sink, thereby resulting in very high roundtrip efficiency.

Jockenhöfer et al. Jockenhöfer *et al.* (2018) studied the coupling of low temperature heat sources with PTES. They developed a numerical model for a subcritical PTES system working with butene and found that the ratio of supplied electrical power to useful electrical power is 1.25 with a maximum exergetic efficiency of 59%, operating between a source and sink temperature of 100°C and 15°C respectively. If the thermal energy is not utilized, the maximum exergetic efficiency drops to 52%.

The studies conducted so far focus on the performance of the coupled high temperature heat pump (HT-HP), TES and heat engine system. The current work, however, concentrates on the evaluation of an organic Rankine cycle (ORC) as a heat engine to produce power in a CHEST system and the technical challenges involved in its integration. This work is part of the H2020 CHESTER (Compressed Heat Energy STorage for Energy from Renewable sources) project Chester (2018). This project proposes the development of a PTES system that couples a TES system with a subcritical HT-HP in the charging-side and an ORC in the discharging-side. Investigations focused on the challenges associated with the integration of a heat engine in such a Carnot battery has not been carried out in the literature to the best of the author's knowledge. Although several concepts have been proposed for Carnot Batteries, there are no laboratory or plant scale demonstration facilities that provide the energy storage community with scientific data.

2. PRELIMINARY WORKING FLUID SELECTION

The selection of the working fluid is crucial to achieve maximal engine thermal efficiency and power. This will be a key point as the cost competitiveness of the CHEST system heavily depends on the roundtrip efficiency that can be achieved.

The working fluids under consideration will need to work under a predefined set of constraints related to the challenges in the CHESTER project. These constraints correspond to a maximum evaporation temperature of 133°C, minimum condensation temperature of 0°C and an ASHRAE toxicity and flammability of A and 2L or less respectively. Also the GWP (Global Warming Potential) and ODP (Ozone Depletion Potential) must be less than 150 and 0 respectively. A pressure drop of 20 kPa or higher would also be important. A number of potentially promising working fluids were examined for this cause. Table 1 lists the different working fluids studied for their chemical properties such as toxicity, flammability, GWP and ozone depletion potential (ODP). The data on toxicity, flammability, GWP and ODP are retrieved from the ASHRAE database whenever available. From Table 1, it is seen that many suitable hydrocarbons have a very high GWP and a non-zero ODP and hence these refrigerants will not be be considered for the project. On the other hand, hydro-fluoro-olefins (HFOs) are characterized by very low GWP and zero ODP.

Table 1: Working fluid chemical properties and output power relative to R245fa.

Refrigerant	Toxicity	Flammability	GWP	ODP	Δp	P_{rel}
R114	A	1	3.9	1	18.77	1.08
R1234ze(Z)	N.A.	N.A.	<10	0	18.79	1.08
R124	B	1	610	0.03	31.46	1.51
R13l1	N.A.	1	1	0	33.1	1.12
R142b	N.A.	N.A.	2270	0.065	27.15	1.15
R236ea	B	1	1200	0	22.03	1.23
R245fa	B	1	1030	0	18.07	1
R40	A	3	13	0.02	41.04	0.91
R600	A	3	20	0	20.04	1.12
R600a	B	3	3.3	0	25.36	1.23
RE245cb2	N.A.	N.A.	N.A.	N.A.	20.53	1.32
HFO-1336mzz(E)	B	1	32	0	20.95	1.42
HFO-1336mzz(Z)	B	1	9.4	0	10.41	1.07
R1233zd(E)	A	1	1	0	14.67	0.51
R1224yd	N.A.	1	1	0	16.24	0.80
R1234yf	A	2L	1	0	**	-

Thermodynamic simulations were carried out in Engineering Equation Solver (EES) to rank the performance of the working fluids based on the specific power output and to determine the pressure drop over the expander as detailed in Table 1. The manufacturer of the reciprocating expander recommends a pressure drop (Δp) of 20 bar over the expander. This is in order to reduce leakage losses and to increase isentropic efficiency Bouvier *et al.* (2016). A higher pressure will enforce a better sealing at both the inlet valve and the piston ring. Additionally, the isentropic efficiency will increase as the work output is increased assuming stable mechanical and electrical losses. Power relative to that obtained when using the cycle for the refrigerant R245fa is reported. Of the HFOs studied, R1234ze(Z) and HFO-1336mzz(E) are found to be the most promising working fluids that operate within the constraints of the project, while meeting the performance required for the expander and the ORC.

Subsequently, based on these results, a detailed cycle analysis is presented in the next section for both R1234ze(Z) and HFO-1336mzz(E). This nominal point includes the mass flow rate of the working fluid, the temperature at the inlet of the expander, the heat supplied to the fluid in the evaporator and the work output from the expander and the overall efficiency of the ORC.

3. MODEL DESCRIPTION

The thermodynamic model of the ORC was developed in Python v3.6.0 Python (n.d.). Working fluid thermodynamic properties were called from the reference fluid property database REFPROP v10 Lemmon *et al.* (n.d.). The pressures and inlet temperatures of the hot and cold fluid in the heat exchangers are set to 900 kPa, 100 kPa and 406 k respectively. The degree of subcooling and superheating is 3 k and 5 K respectively with the condenser outlet temperature of 310 K. A non-linear interior point optimization solver called IPOPT Wächter & Biegler (2006) is utilized to solve a system of equations with the unknown temperatures and pinch points as variable. With the obtained values, mass flow rates of the working fluid and of the hot and cold fluid are calculated.

An exergy analysis proceeds these calculations Long *et al.* (2014).

The exergy destruction in the evaporator ($\dot{I}_{lat}$), preheater ($\dot{I}_{sen}$) and the condenser ($\dot{I}_{cond}$) is given as:

$$\dot{I}_{lat} = \left(1 - \frac{T_0}{T_9}\right)\dot{Q}_{lat} - \dot{E}_{in,lat} \tag{1}$$

Table 2: Work and heat interaction results, exergy analysis and exergy destruction ratio for different components of the ORC for working fluids HFO-1336mzz(E), R1234ze(Z) and R245fa.

Property	HFO-1336mzz(E)	R1234ze(Z)	R245fa
$\dot{Q}_{lat}$	68.53 kW	121.62 kW	117.02
$\dot{Q}_{sen}$	118.86 kW	126.49 kW	128.17
$\dot{Q}_{cond}$	171.98 kW	225.63 kW	223.4
W_{net}	14.21 kW	21.93 kW	20.59
η_{cyc}	7.58%	8.83%	8.4%
$\dot{I}_{lat}$	2.15 kW	2.37 kW	2.26 kW
$\dot{I}_{sen}$	0.97 kW	1.54 kW	1.69 kW
$\dot{I}_{cond}$	6.41 kW	15.18 kW	10.97 kW
$\dot{I}_{exp}$	9.94 kW	14.57 kW	13.56 kW
$\dot{I}_{tot}$	19.42 kW	33.66 kW	28.48 kW
$\dot{E}_{in}$	43.68 kW	60.58 kW	59.53kW
η_{ex}	35.30%	37.12%	36.6%
$y_{D,lat}$	4.92%	3.19%	3.79%
$y_{D,sen}$	2.22%	2.54%	2.83%
$y_{D,cond}$	14.67%	25.05%	18.42%
$y_{D,exp}$	22.75%	24.06%	22.77%
Total	44.56%	54.84%	47.81%

$$\dot{I}_{sen} = T_0[\dot{m}_{wf}(s_4 - s_3) - \dot{m}_{hf,sen}(s_{11} - s_{12})] \tag{2}$$

$$\dot{I}_{cond} = T_0[\dot{m}_{wf}(s_7 - s_2) - \dot{m}_{cf}(s_{14} - s_{13})] \tag{3}$$

Exergy destroyed in the expander is given as:

$$\dot{I}_{exp} = T_0[\dot{m}_{wf}(s_7 - s_6)] \tag{4}$$

Exergy rate transferred to the working fluid is given as:

$$\dot{E}_{in} = \dot{m}_{hf,sen}[(h_{11} - h_{12}) - T_0(s_{11} - s_{12})] \tag{5}$$

The total exergy destroyed in the ORC is:

$$\dot{I}_{tot} = \dot{I}_{lat} + \dot{I}_{sen} + \dot{I}_{cond} + \dot{I}_{exp} \tag{6}$$

The overall exergy efficiency is given as:

$$\eta_{ex} = \frac{W_{turb} - W_{pump}}{\dot{E}_{in}} \tag{7}$$

The exergy destruction ratio, as defined in Lecompte *et al.* (2014), is given as:

$$y_{D,component} = \frac{\dot{I}_{component}}{\dot{E}_{in}} \tag{8}$$

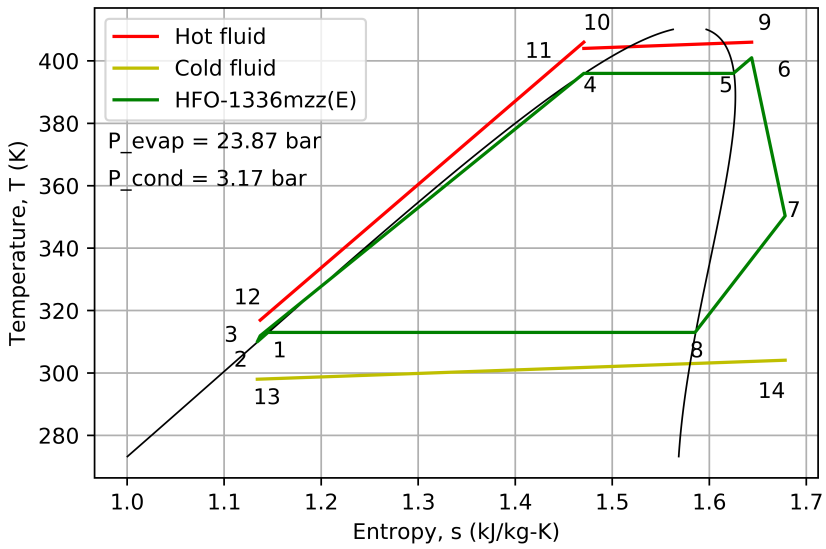

(a) T-s plot of the ORC with HFO-1336mzz(E) as working fluid.

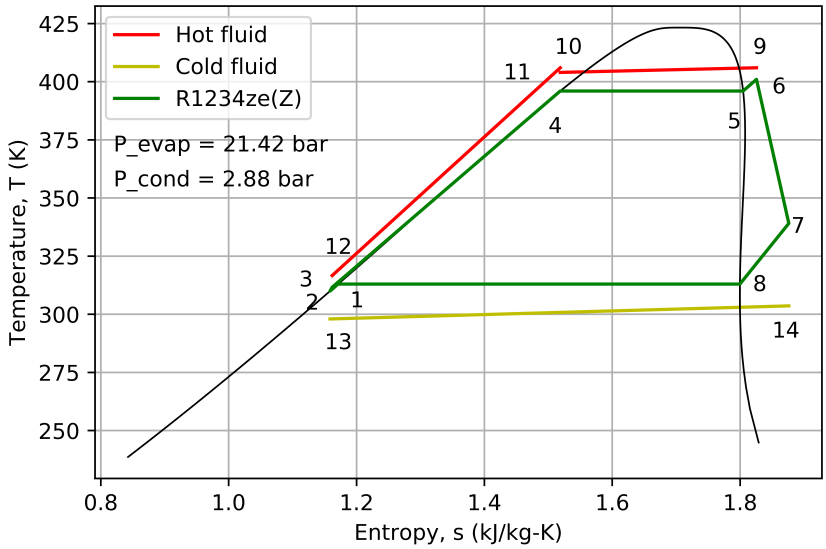

(b) T-s plot of the ORC with R1234ze(Z) as working fluid.

Figure 1: T-s plot of the ORC with different working fluid.

where, T_0 is the reference temperature equal to 288 K, $\dot{I}_{component}$ is the exergy destruction of a given component, $\dot{m}_{wf}$ is the mass flow rate of the working fluid, $\dot{m}_{hf,lat}$, $\dot{m}_{hf,sen}$ and $\dot{m}_{cf}$ is the mass flow rate of the hot fluid in the latent and sensible heat evaporator and that of the cold fluid respectively, W_{turb} the turbine work and W_{pump} the pump work and W_{net} is pump work subtracted from the turbine work. The cycle efficiency defined as the ratio of net work to the total heat input to the latent and sensible evaporators.

4. RESULTS AND DISCUSSION

The T-s diagrams of the ORC system working within the defined constraints are presented in the Figures 1a and 1b. The plot shows the results of the simulation carried out between an evaporator pressure of 23.87 bar and a condenser pressure of 3.17 bar for HFO-1336mzz(E) and an evaporator pressure of 21.42 bar and a condenser pressure of 2.88 bar for R1234ze(Z).

The use of two different heating system results in a better match between the thermal profiles of the working fluid and the TES system, as can be seen in the T-s plots. The heat required in the sensible ($\dot{Q}_{sen}$) and latent ($\dot{Q}_{lat}$) heat TES is given in Table 2 together with the value of heat rejected to the condenser ($\dot{Q}_{cond}$) and the value of the net power output. Using these values, the efficiency of the ORC system is calculated and is found to be 7.58% with HFO-1336mzz(E) and 8.83% with R1234ze(Z) as the working fluid, while its is 8.4% for R245fa. The heat transferred from the PCM to the working fluid needs to be twice as high when R1234ze(Z) is used as a working fluid compared to the heat transferred with HFO-1336mzz(E), for the same mass flow rate. The efficiency achieved by these two cycles is nearly the same. This means that for a fixed capacity of sensible heat storage much larger PCM storage is needed for R1234ze(Z) compared to HFO-1336mzz(E). The ratio of latent heat transfer rate to the sensible heat transfer rate for R1234ze(Z) is 0.96, whereas for HFO-1336mzz(E) it is 0.57. For a unit mass flow rate of the working fluid, the net power obtained from the cycle for HFO-1336mzz(E) is 14.2 kW and for R1234ze(Z) this is 21.9 kW. The heat transferred in the latent heat evaporator increased by 77% with the use of R1234ze(Z), but the net work obtained also increased by 54%.

Table 1. lists the results of exergy analysis performed for both the selected working fluids. The total exergy destroyed increases by 73% if the working fluid used is R1234ze(Z) and by 46% if R245fa is used instead of HFO-1336mzz(E). With approximately the same exergetic efficiency for both working fluids, the exergy available at the inlet of the heat source is higher for R1234ze(Z) but the losses in exergy are also very high in comparision to HFO-1336mzz(E). Table 1 presents the exergy destruction ratios for different components of the ORC when operated with different working fluids. It can be seen overall that the exergy destruction is most for R1234ze(Z). For each working fluid, the component where exergy was destroyed the most was in the expander, following the condenser and then the evaporator.

Based on the simulation results, for a turbine power output of 10 kW, which is defined by the project constraints, the mass flow rate is found out to be 0.61 kg/s and 0.43 kg/s for HFO-1336mzz(E) and R1234ze(Z) as working fluids respectively. For this nominal point of operation, a preliminary test rig is being developed, the process and instrumentation diagram for which can be found in Figure 2.

5. CONCLUSIONS

A comprehensive study on the selection of an appropriate working fluid was conducted by theoretically testing more than 15 refrigerants in EES. Most of the refrigerants suffered the demerit of being environmentally hazardous, but a few promising refrigerants were shortlisted based on desirable GWP and ODP values. Among them, refrigerants that would perform well within the constraints of the test were selected and were identified as HFO-1336mzz(E) and R1234ze(Z). Their low GWP and zero ODP values, along with a minimum required pressure drop between the evaporator and condenser pressure made them the refrigerants of choice for this study.

A thermodynamic model of an ORC was developed in Python to estimate the work and heat interaction using the selected working fluids considering a combination of sensible and latent heat sources. The cycle efficiency was calculated based on these parameters and were found to be 7.58 % and 8.83 % the working fluids HFO-1336mzz(E) and R1234ze(Z) respectively. The ratio of latent heat transfer rate to the sensible heat transfer rate is higher for R1234ze(Z) resulting in a larger PCM storage.

An exergy analysis was carried out for ORC system and it was found out that the exergy available at the inlet of the heat source for R1234ze(Z) was 38% more when compared to that available for HFO-1336mzz(E). But, with approximately the same exergetic efficiency of the cycle, the total destruction of exergy is 44% more when the selected working fluid is R1234ze(Z). Calculation of exergy destruction ratio revealed that most of the exergy was destroyed in the expander and the condenser, whereas, the overall exergy destruction was most for the working fluid R1234ze(Z) and the least for HFO-1336mzz(E).

Based on this preliminary analysis the sizing of the components for the ORC prototype has been made.

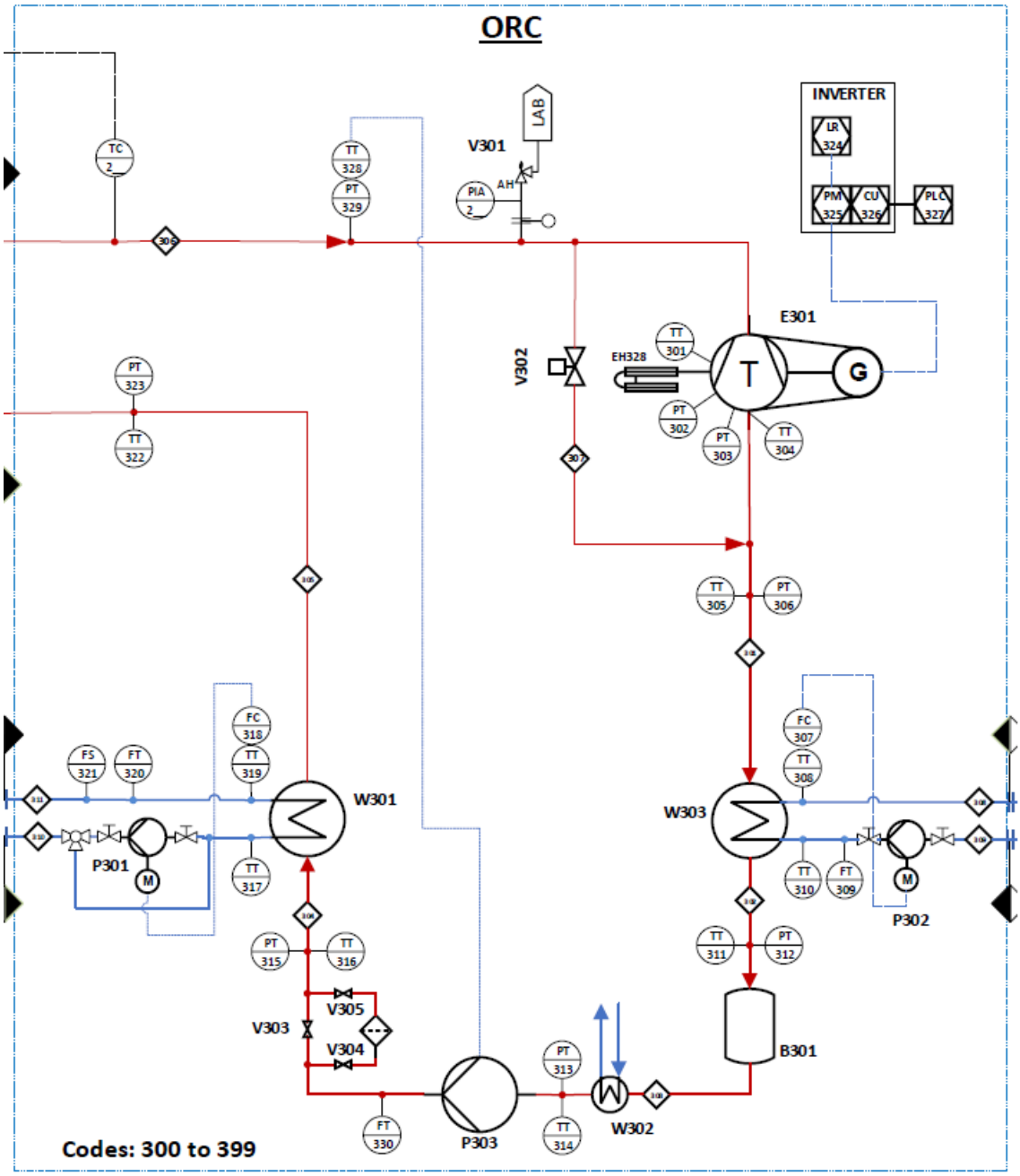

Figure 2: Process and instrumentation diagram of the proposed experimental setup.

The next step of this research will be an experimental campaign to investigate how the ORC behaves with various heat inputs followed by an overall system test including heat pump and thermal storage system.

NOMENCLATURE

W	Work transfer rate	(kW)	**Subscript**	
$\dot{Q}$	Heat transfer rate	(kW)	exp	expander
η	Efficiency		cond	condenser
$\dot{E}$	Inlet exergy	(kW)	lat	latent
$\dot{I}$	Irreversibility	(kW)	sen	sensible
h	Specific enthalpy	(kJ/kg)	turb	turbine
s	Specific entropy	(kJ/kg-K)	hf	hot fluid
T_0	Reference temperature	(K)	cf	cold fluid
p	Pressure	(kPa)	wf	working fluid
			wf	working fluid
			in	inlet
			tot	total
			ex	exergy

REFERENCES

Akhil, Abbas A, Huff, Georgianne, Currier, Aileen B, Kaun, Benjamin C, Rastler, Dan M, Chen, Stella Bingqing, Cotter, Andrew L, Bradshaw, Dale T, & Gauntlett, William D. 2013. *DOE/EPRI 2013 electricity storage handbook in collaboration with NRECA*. Sandia National Laboratories Albuquerque, NM.

Bouvier, Jean-Louis, Lemort, Vincent, Michaux, Ghislain, Salagnac, Patrick, & Kientz, Thiebaut. 2016. Experimental study of an oil-free steam piston expander for micro-combined heat and power systems. *Applied energy*, **169**, 788–798.

Chester. 2018. *COMPRESSED HEAT ENERGY STORAGE FOR ENERGY FROM RENEWABLE SOURCES*. `https://www.chester-project.eu/`. Accessed: 2019-04-15.

Connolly, David, Lund, Henrik, Mathiesen, Brian Vad, Pican, Emmanuel, & Leahy, Martin. 2012. The technical and economic implications of integrating fluctuating renewable energy using energy storage. *Renewable energy*, **43**, 47–60.

Denholm, Paul, & Hand, Maureen. 2011. Grid flexibility and storage required to achieve very high penetration of variable renewable electricity. *Energy Policy*, **39**(3), 1817–1830.

Gallo, AB, Simões-Moreira, JR, Costa, HKM, Santos, MM, & dos Santos, E Moutinho. 2016. Energy storage in the energy transition context: A technology review. *Renewable and Sustainable Energy Reviews*, **65**, 800–822.

Gutiérrez, Marcos, & Arántegui, Roberto. 2015. Assessment of the European potential for pumped hydropower energy storage based on two existing reservoirs. *Renewable energy*, **75**, 856–868.

Inage, Shin-ichi. 2015. The role of large-scale energy storage under high shares of renewable energy. *Wiley Interdisciplinary Reviews: Energy and Environment*, **4**(1), 115–132.

IRENA. 2012. *Electricity storage technology brief IEA-ETSAP and IRENA technology policy brief E18; 2012*. `https://www.irena.org/DocumentDownloads/Publications/IRENA-ETSAP%20Tech%20Brief%20E18%20Electricity-Storage.pdf`. Accessed: 2019-04-15.

Jockenhöfer, Henning, Steinmann, Wolf-Dieter, & Bauer, Dan. 2018. Detailed numerical investigation of a pumped thermal energy storage with low temperature heat integration. *Energy*, **145**, 665–676.

Lecompte, Steven, Ameel, Bernd, Ziviani, Davide, van den Broek, Martijn, & De Paepe, Michel. 2014. Exergy analysis of zeotropic mixtures as working fluids in Organic Rankine Cycles. *Energy Conversion and Management*, **85**, 727–739.

Lemmon, E.W., Bell, I.H., Huber, M.L., & McLinden, M.O. *REFPROP Reference Fluid Thermodynamic and Transport Properties*. `https://www.nist.gov/srd/refprop`, year = 2018, note = Accessed: 2019-04-15,.

Long, R, Bao, YJ, Huang, XM, & Liu, W. 2014. Exergy analysis and working fluid selection of organic Rankine cycle for low grade waste heat recovery. *Energy*, **73**, 475–483.

Müller, Marcus, Viernstein, Lorenz, Truong, Cong Nam, Eiting, Andreas, Hesse, Holger C, Witzmann, Rolf, & Jossen, Andreas. 2017. Evaluation of grid-level adaptability for stationary battery energy storage system applications in Europe. *Journal of Energy Storage*, **9**, 1–11.

Python. *Python programming language*. `https://www.python.org/`, year = 2016, note = Accessed: 2019-04-15,.

Steinmann, WD. 2014. The CHEST (Compressed Heat Energy STorage) concept for facility scale thermo mechanical energy storage. *Energy*, **69**, 543–552.

Wächter, Andreas, & Biegler, Lorenz T. 2006. On the implementation of an interior-point filter line-search algorithm for large-scale nonlinear programming. *Mathematical programming*, **106**(1), 25–57.

Zhu, Qian. 2015. *High-efficiency power generation–review of alternative systems*.

ACKNOWLEDGEMENT

This work has been partially funded by the grant agreement No. 764042 (CHESTER project) of the European Union's Horizon 2020 research and innovation program. We would also like to thank The Chemours Company for providing us with the information on HFO-1336mzz(E).